다자유도 구면 동력장치의 설계 및 제어를 위한 토크 해석
Torque for Design and Control of a Spherical Actuator

*#손흥선 [1], 송준엽 [2], Kok-meng Lee[3]
*#Hungsun Son[1](hson@kimm.re.kr), Jun Yeob Song[2],
[1,2] 한국 기계연구원, [3] Georgia Institute of Technology

Key words : Magnetic field, dipole, torque model, actuator design, stepper control

1. Introduction

Recently, growing demands for miniature devices in modern industries such as micro-machining of biomedical and optical components along with the trend to downscale equipments have motivated the development of novel actuators for dexterous stages capable of precision machining complex-shaped objects. Such systems often need multi-degree of freedom (DOF) manipulation of the cutter or stage orientation. Existing multi-DOF rotational stages typically use a combination of single-axis actuators to control orientation. Driven by the stringent accuracy and tolerance requirements, various forms of micro-motion parallel mechanisms with three or more single-axis actuators were developed. Although these multi-DOF mechanisms are structurally more rigid, they are bulky, require more passive joints than the number of DOF of the stage, and offer very limited motion range. Unlike many existing orientation stages, ball-joint-like actuators [1] (capable of three-DOF orientation in a single joint) offer an attractive alternative to eliminate motion singularities of the multi-DOF rotational stage.

Design and control of multi-DOF electromagnetic actuators require a good understanding of the magnetic fields, and involve real-time calculation of magnetic forces. Numerical methods (such as FEM) are computationally expensive for design optimization or real-time control. Due to the lack of efficient computational methods for magnetic fields and forces/torques, a number of researchers have resorted to simple empirical lumped-parameter models that often offer only first order accuracy. An alternative method has been based on the concept of a magnetic dipole originally suggested by Fitz Gerlad in 1883 as a tool to characterize potential fields. While the dipole model has been widely used to analyze the magnetic field at a sufficiently large distance for applications such as electromagnetic wave propagation (antenna dynamics) and geomagnetism (earth polarization), it generally gives a poor approximation when the length scale of the field is very small such as in an air-gap of a actuator. For reasons including compact formulation/solutions and intuitive magnetic fields, many researchers continue to develop dipole models for analyzing actuator designs involving permanent magnets. Nedelcu et al. [2] used a magnetic dipole model to describe the field of a PM-based device, where each PM is modeled as a doublet. The existing single dipole model, which bases on the mathematical theory of a doublet, is often studied in the context of physics and valid only for needle-like magnets; thus, it has very limited applications in modern actuator designs.

2. Magnetic Field Model

Magnetic forces involved in a spherical actuator can be generally calculated using the Lorenz force equation:

$$\mathbf{F} = -\oint \mathbf{B} \times Id\boldsymbol{\ell} \qquad \text{where} \quad I = -\iint \mathbf{J} \bullet d\mathbf{S} \qquad \text{(1a,b)}$$

where **B** is the magnetic field vector; I is current vector through the conductor; and $\boldsymbol{\ell}$ is the normalized vector of the current direction. In (1b), the current density vector J is directly used in the calculation and thus, it is not necessary to compute the magnetic flux generated by the current loop. Thus, the Lorenz force calculation involves only the B-fields of the permanent magnets. The magnetic field B of the rotor PM's in (1a, b) can be first computed. For this, we model the PM using the concept of distributed multiple poles (DMP) [3]. This DMP method provides us a means to derive closed-form solutions for characterizing the magnetic field B that satisfies the following assumptions: the field is continuous and irrotational; and the medium is homogeneous. These enable us to define a scalar magnetic potential Φ such that the magnetic field intensity H given by

$$\mathbf{H} = -\nabla\Phi \quad \text{and} \; \mathbf{B} = \mu_0 \mathbf{H} \qquad (2)$$

satisfies $\nabla^2\Phi = 0$. The solution to Laplace's equation, which satisfies the field for a magnetic pole, is given by

$$\Phi = \frac{(-1)^j}{4\pi R} m \qquad (3)$$

where *m* is the strength of the pole; *j* takes the value 0 or 1 designating that the pole is a source or a sink respectively; and *R* is the distance from the pole to the field point. Since a single pole does not exist alone in a physical magnet filed, we define a dipole here as a pair of source and sink separated by a distance $\bar{\ell}$.

To account for the shape of a physical magnet, we illustrate the model of a cylindrical magnet with radius *a*, length ℓ and $\mathbf{M} = M_o \mathbf{e}_z$) using multiple dipoles as shown in Fig. 3, where *k* circular loops (each with radius $\bar{a}_j$) of *n* dipoles are uniformly spaced in parallel to the magnetization vector.

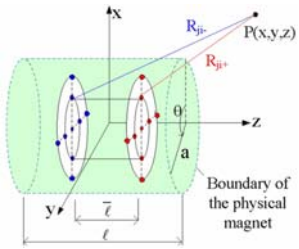

Fig. 1 DMP model of a cylindrical magnet

In Fig. 1, R_{ji+} and R_{ji-} , which are the distances from the i^{th} pair of source and sink in the j^{th} loop to any point P(x,y,z):

$$R_{ji\pm}^2 = \left[x - \bar{a}_j \cos i\theta\right]^2 + \left[y - \bar{a}_j \sin i\theta\right]^2 + \left(z \mp \bar{\ell}/2\right)^2 \qquad (4)$$

where $j = 0,1,...,k$; $\bar{a}_j = aj/(k+1)$; and $0 < \bar{\ell} < \ell$. Combined with (2) and (3), the total net field of a PM can be deduced as the second order linear partial differential equation which is the Laplace equation. Therefore, the magnetic field Φ(x,y,z) of the PM can be obtained by summing the magnetic fields contributed by the individual poles: Equations (2), (3) and (4) offer a closed-form solution to determine the three dimensional (3D) magnetic field of a PM. The total field **B** can be obtained from the vector sum of the individual fields. A general expression of the magnetic field of a PM can be expressed as

$$\Phi = \frac{1}{4\pi} \sum_{j=0}^{k} m_j \sum_{i=1}^{n_k} \left(\frac{1}{R_{ji+}} - \frac{1}{R_{ji-}} \right) \qquad (5)$$

where $n_k = 1$, n for $j = 0$, $j \neq 0$ respectively and the method to

determine modeling parameters (k, n, $\bar{\ell}$, and m_j where $j = 0, \ldots, k$) is shown in [3].

Once the field distribution is computed, the force and torque on the boundary of the moving magnet can be calculated from (1a) and (1b) respectively.

3. DESIGN AND OPERATIONAL PRINCIPLE

Figure 2 illustrates the design concept of spherical actuators, which consist of two functional subsystems; a PM-based rotor system, and an electromagnetic (EM) regulator to control the rotor orientation.

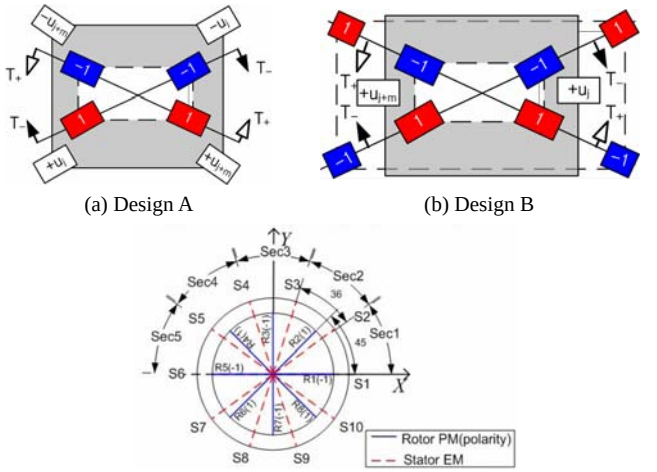

(a) Design A (b) Design B

(c) Top view of PM and EM pole-pairs

Fig. 2 Design concept of spherical actuators

Both of Design A and B consist of two layers of PM and EM pairs in Fig. 2(a) and (b). There are 10 stator EMs and 8 rotor PM pole-pairs (PMpp's) in each layer for Design A but 16 PMpp's for Design B since the rotor PMs in Design A are only inside the stator EM pole-pairs (EMpp's) and Design B are both inside and outside the stator EMpp's in Fig 2 (c). The EMpp's are arranged in pairs on a plane perpendicular to the XY plane and point radially towards the stator center. The EM polarities can be externally controlled. Due to the page limit, we denote the number of PMpp's and EMpp's as m_r and m_s and discuss only the ZX plane of PMpp's and EMpp's from here on. As shown in Fig. 2 (a) and (b), the main difference of two designs is the number of layers of rotor PMpp's. The conventional design like design A only uses the field interaction of both rotor PMs and stator EMs in one side of air-gap region. However, the proposed design will facilitate the both sides (inside and outside) of the air-gap like design B. Since one side of PMpp's is different from the other side, the both ends of electromagnets interact with the PMpp's simultaneously shown in Fig. 3. In addition, for the field distribution, Design B has less leakage magnetic field than Design A. Thus, the torque generated by the same amount of current is about twice stronger as shown in Fig 4. The simulation parameters are detailed in Table 1 where both coils are energized with different polarities to generate the same direction of torque.

Table 1 Values used in the setup

Rotor radius	50.8mm (2 inches)
Air gap	0.7mm (0.03inch)
Stator EM's	20 (2 layers of 10)
Magnetization angles	$\gamma_s = 26^o$; $\delta_s = 36^o$
Current per pole-pair (A)	$u_j = 2$, $u_j = -2$
Rotor PM's (A/B)	16 / 32 (2 layers of 8/16)
Magnetization $\mu_0 M_0$	1.35T
Magnetization angles	$\gamma_r = 20^o$; $\delta_r = 45^o$

Based on the torque of the spherical actuator, the operation principle for the control of the rotor can be developed. The Spherical actuator operates in two different modes; static rotor orientation control and orientation control with continuous spinning. The rotor orientation is regulated on the principle of push-pull operation. As illustrated in Figs. 2(a) and (b), the inclination from the Z-axis is manipulated using two opposing torques, T_+ and T_-, about the axis normal to the plane that contains the current inputs u_j and u_{j+m} producing the torques.The torque model represents a 'holding torque' to maintain the rotor shaft at a particular inclination. The specific polarities of the EMpp's depend on the PMpp's layout; for example, $u_j = u_{j+m}$ to maintain the rotor at zero inclination. Any perturbation will result in a differential torque ΔT driving the rotor to its equilibrium. Thus, the torque ΔT represents the 'driving torque' because it results in the motion of the rotor. For this push-pull operation, the torque model is written in the following form:

$$\mathbf{T} = \mathbf{T}_+ + \mathbf{T}_- + \Delta\mathbf{T} \tag{6}$$

4. CONCLUSIONS

We presented the design concept, model and basic operation principle, and showed how the orientation of the Spherical actuator can be controlled. We have also reviewed the DMP modeling method and derived closed form solutions to characterize the magnetic fields, from which the magnetic force and torque are derived using the Lorenz force equation.

Two design concepts of the spherical actuator have been demonstrated at no load to compare their torque. With the same amount of current vector, the torque generated by the design B is significantly stronger. However, preliminary results presented here did not take into account the motor and load dynamics, which could result in phase lag during transient. It is expected that these dynamic effects can be compensated using feedback control, a research topic being investigated.

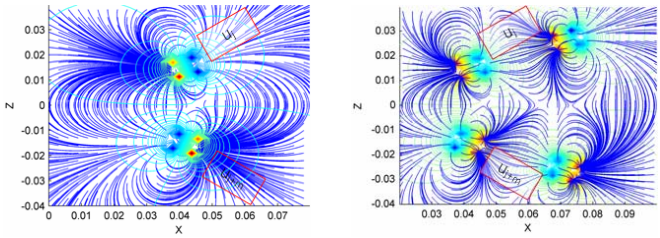

(a) Design A (a) Design B

Fig. 3 Magnetic field of both design A and B

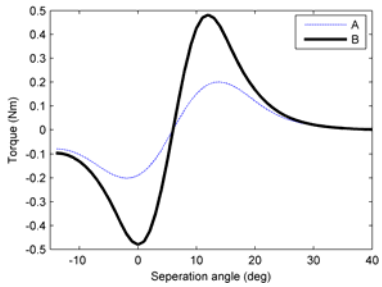

Fig. 4 Torque comparison of both design A and B

References

1. K.-M. Lee and C. Kwan, "Design concept development of a spherical stepper for robotic applications," IEEE Trans. Robot. Autom., vol. 7, no. 1, pp. 175–181, Feb. 1991.
2. S. Nedelcu and J. H. P. Watson, "Magnetic dipole model of a permanent magnet based device," J. Phys., vol. 34, no. 17, pp. 2622–2628, Sep. 2001.
3. K.-M. Lee and H. Son, "Distributed multipole model for design of permanent-magnet-based actuators," IEEE Trans. Magn., vol. 43, no. 10, pp. 3904–3913, Oct. 2007.